

## Delineating a shallow fault zone and dipping bedrock strata using multichannel analysis of surface waves with a land streamer

Julian Ivanov<sup>1</sup>, Richard D. Miller<sup>1</sup>, Pierre Lacombe<sup>2</sup>, Carole D. Johnson<sup>3</sup>, and John W. Lane Jr.<sup>3</sup>

### ABSTRACT

The multichannel analysis of surface waves (MASW) seismic method was used to delineate a fault zone and gently dipping sedimentary bedrock at a site overlain by several meters of regolith. Seismic data were collected rapidly and inexpensively using a towed 30-channel land streamer and a rubberband-accelerated weight-drop seismic source. Data processed using the MASW method imaged the subsurface to a depth of about 20 m and allowed detection of the overburden, gross bedding features, and fault zone. The fault zone was characterized by a lower shear-wave velocity ( $V_s$ ) than the competent bedrock, consistent with a large-scale fault, secondary fractures, and in-situ weathering. The MASW 2D  $V_s$  section was further interpreted to identify dipping beds consistent with local geologic mapping. Mapping of shallow-fault zones and dipping sedimentary rock substantially extends the applications of the MASW method.

### INTRODUCTION

Fault zones can be inferred from offsets in seismic reflections or refractions, scatter or diffraction of seismic waves from beds terminated by a fault plane, or changes in seismic properties across the fault zone. Acquisition and analysis of the reflective and refractive wavefield with one field deployment and component-specific processing allows unique, and in some cases redundant, determination of key seismic characteristics in a time- and cost-effective manner. Methods and approaches using reflections, first arrivals, diffractions, and scatter to map faults are well documented (Romberg, 1952; Castagna, 1995; Hairth and Nawawi, 2000; Demanet et al., 2001). The multichannel analysis of surface waves (MASW) meth-

od has recently been applied to detect a wide range of subsurface features. The MASW method was used to map bedrock at 1.5 to 7 m below land surface, with less than 0.3 m difference from boring data, at a site in Olathe, Kansas (Miller et al., 1999a). Sinkholes and related subsidence features, obscured by suburban development and not detectable using other geophysical methods because of power-line and mechanical noise, reinforced concrete, and noninvasive testing requirements, were identified in a residential area in western Florida (Miller et al., 1999b). Buried pits and trenches were located at an old refinery site in eastern Illinois through coincident analysis of phase and amplitude distortions on surface-wave data (Miller et al., 2000). Tunnels used for trafficking contraband across the U. S. border were detected by analysis of surface-wave scatter caused by the void space of the tunnel (Ivanov et al., 2003).

Recently developed seismic acquisition and analysis methods permit the use of surface waves for investigating near-surface structure, especially structural features characterized by lateral seismic-velocity changes. Surface waves (usually ranging from 5–20 Hz to 50–90 Hz) have proven sensitive to geologic discontinuities at depths ranging from 1 m to > 50 m. This sensitivity can be exploited using site-specific acquisition and processing routines developed for reconnaissance and delineation surveys. Field tests have shown that receiver coupling suitable for accurate recording of surface waves can be obtained by pressure contact to the earth surface, unlike body-wave surveying, in which coupling is optimized by invasive “planting” (Miller et al., 1999a). Marine streamer technology adapted to land provides near-continuous acquisition of 2D profiles using pressure-coupled sources and receivers to result in rapid, less labor-intensive data collection than traditional body-wave reflection methods.

### Survey objectives

The survey objectives were to evaluate the MASW seismic method to map a known fault zone at depths of less than 20 m beneath

Manuscript received by the Editor February 16, 2006; revised manuscript received April 17, 2006; published online August 28, 2006.

<sup>1</sup>The University of Kansas, Kansas Geological Survey, 1930 Constant Avenue, Lawrence, Kansas 66047. E-mail: jivanov@kgs.ku.edu; rmiller@kgs.ku.edu.

<sup>2</sup>U. S. Geological Survey, Toxic Substances Hydrology Program, 810 Bear Tavern Road, Suit 206, West Trenton, New Jersey 08628. E-mail: placombe@usgs.gov.

<sup>3</sup>U. S. Geological Survey, OGW, Branch of Geophysics, 11 Sherman Place, Unit 5015, Storrs, Connecticut 06269. E-mail: cjohnson@usgs.gov; jwlane@usgs.gov.

© 2006 Society of Exploration Geophysicists. All rights reserved.

weathered material and to evaluate the ability of MASW to detect dipping bedrock strata. This study included a calibration phase to identify the fault “signature” and an exploration phase to search for the subsurface expression of the main fault zone and any secondary features related to faulting at the site.

### Surface-wave inversion

Traditionally, surface waves are viewed as noise in multichannel seismic data for imaging shallow engineering, environmental, groundwater, and geologic features (Steeple and Miller, 1990). Recent developments permit interpretation of surface-wave data by combining spectral analysis of surface waves (SASW) methods developed for civil-engineering applications (Nazarian et al., 1983) with multitrace reflection methods developed for near-surface (Schepers, 1975) and petroleum applications (Glover, 1959). The combination of these two approaches permits noninvasive estimation of shear-wave velocity ( $V_s$ ) and delineation of horizontal and vertical variations in near-surface material properties using the MASW method (Park et al., 1999; Xia et al., 1999).

Surface-wave travel (through the shallow layers of the earth) is controlled primarily by the  $V_s$  and layer geometry (Xia et al., 1999). Because surface waves are dispersive, the dispersion curve relating frequency and phase velocity can be inverted to estimate  $V_s$  as a function of depth.

The MASW method has effectively detected seismic velocity anomalies at depths of 1.5 to 100 m and noninvasively measured  $V_s$  to within 15% of borehole-measured  $V_s$  (Xia et al., 2000). MASW seismic data are acquired at shot stations evenly spaced along a continuous transect. For each shot station, the surface-wave dispersion curve is inverted to produce a 1D  $V_s$  profile (Park et al., 1999); using commercially available contouring software, a series of profiles is displayed to represent the pseudo 2D  $V_s$  section beneath the transect.

Subsurface seismic anomalies are interpreted in the 2D contoured  $V_s$  field as changes in earth materials or geologic structure.

### Geologic setting

The study area is located in the southeastern part of the Newark Basin adjacent to the former Naval Air Warfare Center in West Trenton, New Jersey (Figure 1). The Stockton and Lockatong Formations of Late Triassic age (Owens et al., 1999) underlie the study area. The older Stockton Formation consists of interbedded red to gray sandstone and red mudstones. The Lockatong Formation consists of cyclically bedded, laminated black to dark-gray mudstone and massive light-gray to red mudstone. The differential weathering characteristics of the Stockton and Lockatong Formations result in an undulating bedrock surface. The regional strike of the bedrock in both formations is about 50° northeast. Bedding in outcrops near the study dips from 15° to 25° northwest; however, off-loading and weathering expansion generally increase bedding dip near the land surface. The region has not been glaciated, and the depth to unweathered bedrock ranges from about 5 to 15 m.

In the study area, a 50-m-wide fault zone separates the Stockton and Lockatong Formations (Lacombe 2000, 2002). The fault strike is subparallel to the formation strike with a dip of about 65° southeast. Rocks within the fault zone are intensely weathered; in places the rocks are weathered to clay to depths in excess of 20 m (Lacombe, 2000). The fault acts as a confining unit, inhibiting groundwater flow from the Lockatong to the Stockton Formation. Figure 3a shows a schematic geologic section modified from Lacombe (2000).

### DATA COLLECTION AND PROCESSING

To identify the fault-zone seismic characteristics, the MASW method was tested in an undisturbed area where the fault zone had been mapped. Once the signature of the fault zone was established, additional surveys (not shown) were conducted on the grounds of the former military base where underground utilities and building foundations created many forms of seismic interference.

Using a towed land streamer composed of 30 geophones with 1.2-m spacing and a rubberband-accelerated weight-drop (RAWD) seismic energy source, a full-wavefield seismic data profile was acquired at a control point to optimize the source offset and shot spacing. The acquisition and analysis of this calibration data took about one-half day. Based on this test, the distance from the seismic source to geophone 1 was set to 18.3 m and the shot spacing was set to 2.5 m.

A 760-m seismic traverse was acquired in about 8 hours over a fallow farm field and a groomed soccer field. The seismic traverse was oriented perpendicular to the mapped fault-zone trace and parallel with the bedrock dip direction. Nearby noise sources included a highway and an active railroad and airport. Using the RAWD seis-

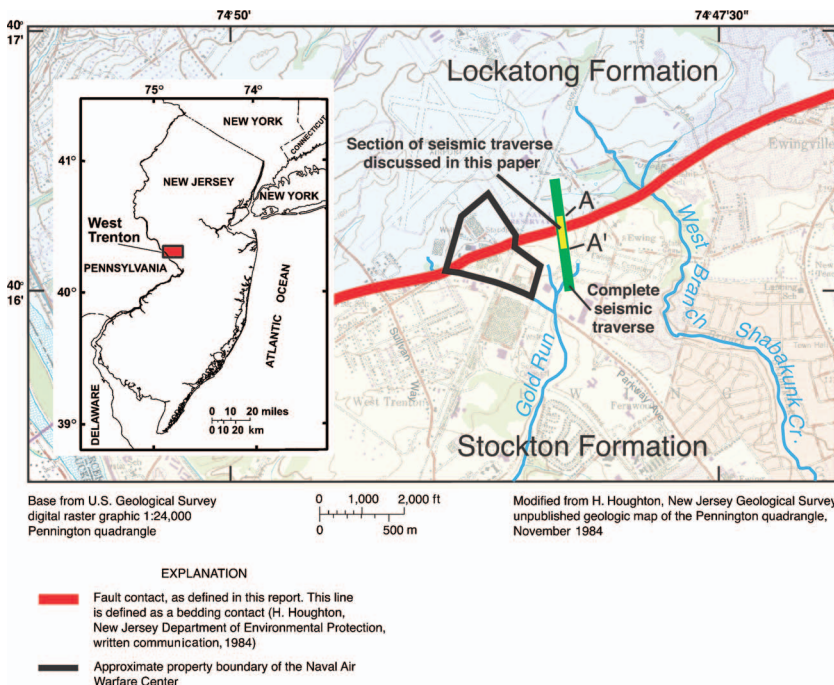


Figure 1. Study area and field site, West Trenton, New Jersey.

mic source and low-frequency geophones, the recorded surface-wave bandwidth ranged from 20 to  $> 80$  Hz; this enabled a 20-m depth of investigation.

The seismic data were analyzed using SurfSeis,<sup>1</sup> a software package from the Kansas Geological Survey. The dispersion curve generated for each shot record was assigned a surface location corresponding to the middle point of its receiver spread. Care was taken to ensure that the spectral properties of the time-distance ( $T$ - $X$ ) data (e.g., time sampling interval, minimum and maximum offsets, etc.) were consistent with the maximum and minimum frequency-phase velocity ( $f$ - $v_p$ ) values of the dispersion curve. On most of the shot records (Figure 2a), surface-wave energy dominates the seismic data, appears moderately dispersive (recognizable as multiples of the surface-wave wavelet), and is coherent. Dispersion-curve images evaluated from such records have a high S/N ratio (Figure 2b). On some of the shot records, the surface-wave energy has smaller apparent velocity, is not as strong, is less coherent, and is noisier (Figure 2c). It is possible that the latter is a result of backscattered energy originating from fractured areas, and these records were interpreted as being from within the fault zone. Corresponding dispersion-curve images have a poorer S/N ratio [estimation of a phase-velocity amplitude with respect to the remaining amplitudes (seismic signals, not related to the estimated trend) at a given frequency; Figure 2b] but sufficient sensitivity to evaluate the dispersion curve trends.

Each dispersion curve was inverted to give a 1D vertical  $V_s$  profile. After inverting all of the dispersion curves, a pseudo-2D  $V_s$  section was produced for the profile line (Figure 3b). Preliminary data processing on site took less than a day to complete; complete processing to produce the profile line in Figure 3b took about 2 weeks.

## 2D SHEAR-WAVE VELOCITY SECTION AND GEOLOGIC SECTION

The 2D  $V_s$  image features (Figure 3b) match well with those from the a priori geologic section (Figure 3a). This close resemblance exceeded our expectations in view of the MASW method uncertainties from 1D inversion nonuniqueness (Xia et al., 1999) and the smearing nature of surface-wave analysis (Xia et al., 2005).

The 2D  $V_s$  section (Figure 3b) shows an 80-m-wide zone between 1300 and 1380 m with seismic velocities ranging from 400–800 m/s. This low-velocity zone coincides with the location of the thrust-fault zone mapped by Lacombe (2002) and is interpreted as the seismic expression of the fault zone (Figure 3c). The low-velocity expression of the fault zone is related to fracturing and associated in-situ weathering that would reduce the shear modulus and, therefore, the  $V_s$  of the faulted strata. Data from drilling at seven sites in the fault zone indicate bedrock in the fault zone is extensively weathered with indurated bedrock

blocks surrounded by clay at depths of up to 60 m. The footwall of the fault zone is expressed as the southeast-dipping velocity anomaly from 1290 to 1300 m.

Figure 3b shows three northwest-dipping, high-velocity regions at 1180–1210 m, 1220–1280 m, and 1380–1450 m. The high-velocity regions ( $> 1000$  m/s) dip about  $10^\circ$  northwest and are interpreted as the seismic expression of the top of highly indurated strata consistent with massive Lockatong Formation mudstones and Stockton Formation sandstones. Above the high-velocity stratum is a mid-velocity stratum with velocities ranging from 600 to 900 m/s and a low-velocity seismic unit that extends from land surface to a depth of about 3–4 m with velocities ranging from 300–600 m/s. The low-velocity stratum is interpreted as soil and highly weathered, shallow bedrock typical of the region.

North of the fault, the mid-velocity stratum in the Lockatong Formation is interpreted as weathered massive and laminated mudstone. South of the fault, the Stockton Formation consists of interbedded sandstone and shale. The sandstone is more indurated, and should

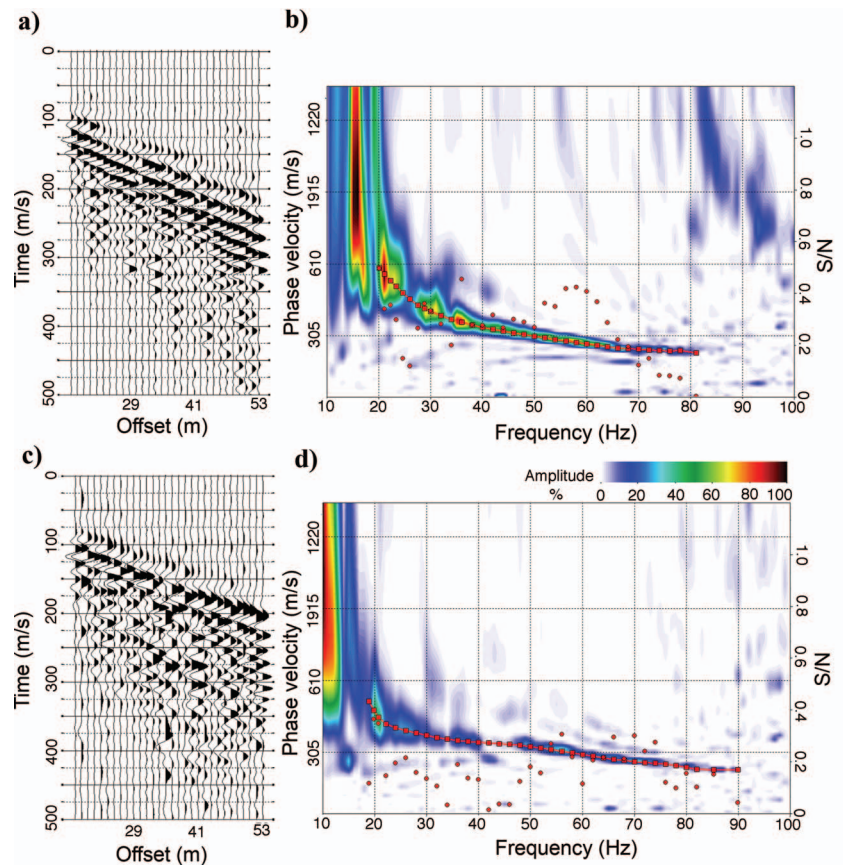


Figure 2. Seismic shot gathers and their corresponding phase-velocity-frequency images: (a) and (b) from an area outside the fault zone with the middle of the spread at 1228 m, and (c) and (d) from an area within the fault zone with the middle of the spread at 1323 m. The dispersion curves [connected red squares on (b) and (d)] were picked following the maximum-amplitude trend; the S/N (right-hand axis; unconnected red circles) can be used to estimate the relative sensitivity of the imaging phase-velocity-frequency method.

<sup>1</sup>Any use of trade, product, or firm names in this paper is for descriptive purposes only and does not imply endorsement by the U. S. Government.

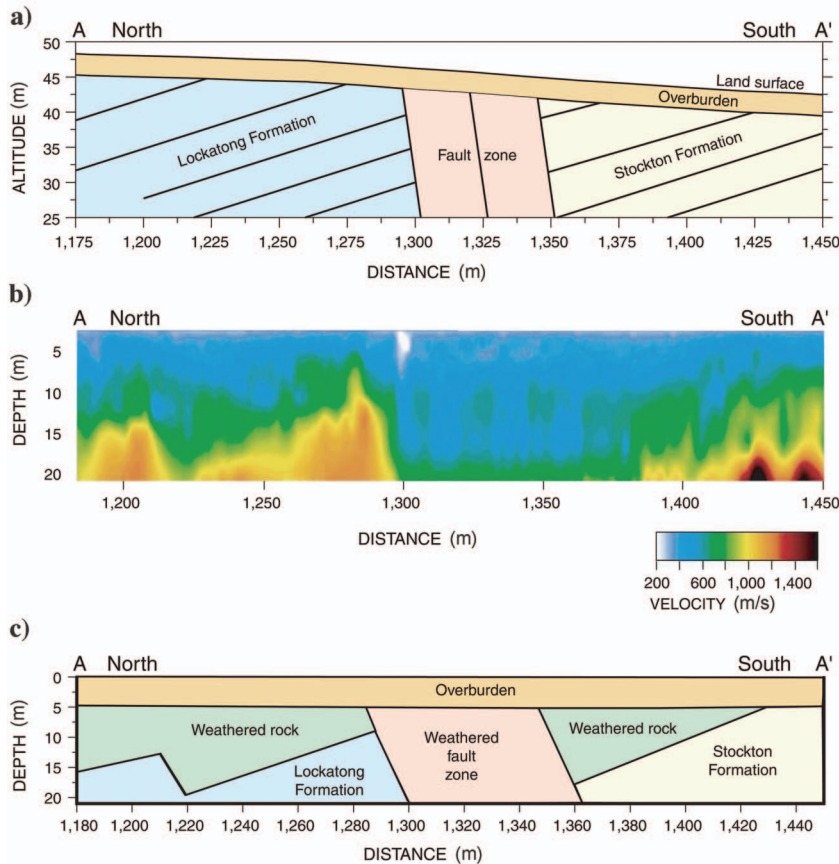


Figure 3. (a) Generalized geologic section for the survey line showing the Lockatong and Stockton Formations separated by a steeply dipping fault zone. (b) Field site of the MASW  $V_p$  section, West Trenton, New Jersey. (c) Interpreted geologic section incorporating the MASW results with the local geology.

have a higher seismic velocity than the shale. The strata with a seismic velocity of 1200 m/s are interpreted as indurated sandstone, and the strata with seismic velocities ranging from 800–1200 m/s are interpreted as shale.

## CONCLUSION

The MASW method was used to map a shallow fault zone and dipping sedimentary bedrock beneath regolith at a site near Trenton, New Jersey. Success at this site was based on effective calibration of the method over an area where the target (fault zone) was known to exist. In this study, the fault zone was detected and uniquely distinguished from dipping bedrock. Delineation of dipping sedimentary bedrock was facilitated by compositionally dependent bedrock-surface weathering. This study has enlarged the range of applications for the MASW method and has shown the efficiency of using the land streamer approach for broadband surface-wave data acquisition.

## ACKNOWLEDGMENTS

The authors thank Jianghai Xia, Mary Brohammer, Peter Joesten, and Alison Waxman for assistance in manuscript preparation and

submission. We appreciate the comments and suggestions of Johan Robertsson, the associate editor, and two anonymous reviewers who have improved the final form of the manuscript. This work was funded by the U. S. Geological Survey Toxic Substances Hydrology Program.

## REFERENCES

- Castagna, J. P., 1995, Intersecting faults, sealing faults, and other exploration issues: *The Leading Edge*, **14**, 1187–1188.
- Demant, D., F. Renardy, K. Vanneste, D. Jongmans, T. Camelbeeck, and M. Meghraoui, 2001, The use of geophysical prospecting for imaging active faults in the Roer Graben, Belgium: *Geophysics*, **66**, 78–89.
- Glover, R. H., 1959, Techniques used in interpreting seismic data in Kansas, in W. W. Hambleton, ed., *Symposium on geophysics in Kansas: Kansas Geological Survey Bulletin*, 137, 225–240.
- Harith, Z. Z. T., and M. N. M. Nawawi, 2000, Mapping faults using seismic refraction and 2D resistivity imaging technique in Kuala Ketil, Malaysia: 62nd Annual International Meeting, EAGE, Extended Abstracts, Session P0112.
- Ivanov, J., R. D. Miller, C. B. Park, and N. Ryden, 2003, Seismic search for underground anomalies: 73rd Annual International Meeting, SEG, Expanded Abstracts, 1223–1226.
- Lacombe, P. J., 2000, Hydrogeologic framework, water levels, and trichloroethylene contamination, Naval Air Warfare Center, West Trenton, New Jersey, 1993–97: U.S. Geological Survey Water-Resources Investigations Report 98–4167.
- , 2002, Ground-water levels and potentiometric surfaces, Naval Air Warfare Center, West Trenton, New Jersey, 2000: U.S. Geological Survey Water-Resources Investigations Report 01–4197.
- Miller, R. D., C. B. Park, J. M. Ivanov, J. Xia, D. R. Lafen, and C. Gratton, 2000, MASW to investigate anomalous near-surface materials at the Indian Refinery in Lawrenceville, Illinois: *Kansas Geological Survey Open-file Report* 2000–4.
- Miller, R. D., J. Xia, C. B. Park, and J. M. Ivanov, 1999a, Multichannel analysis of surface waves to map bedrock: *The Leading Edge*, **18**, 1392–1396.
- , 1999b, MASW to investigate subsidence in the Tampa, Florida area: *Kansas Geological Survey Open-file Report* 99–33.
- Nazarian, S., K. H. Stokoe II, and W. R. Hudson, 1983, Use of spectral analysis of surface waves method for determination of moduli and thicknesses of pavement systems: *Transportation Research Record* 930, 38–45.
- Owens, J. P., P. J. Sugarman, N. F. Sohl, R. A. Parker, H. F. Houghton, R. A. Volkert, A. A. Drake Jr., R. C. Orndorff, L. M. Bybell, G. W. Andrews, D. Bukry, O. S. Zapeecza, G. N. Paulachok, L. Mullikin, 1999, *Bedrock Geologic Map of Central and Southern New Jersey*, U. S. Geological Survey Map I-2540-B.
- Park, C. B., R. D. Miller, and J. Xia, 1999, Multichannel analysis of surface waves (MASW): *Geophysics*, **64**, 800–808.
- Romberg, F., 1952, Limitations of the seismic method of mapping faults: *Geophysics*, **17**, 827–842.
- Schepers, R., 1975, A seismic reflection method for solving engineering problems: *Journal of Geophysics*, **41**, 367–384.
- Steeple, D. W., and R. D. Miller, 1990, Seismic reflection methods applied to engineering, environmental, and groundwater problems, in S. H. Ward, ed., *Investigations in geophysics: Review and tutorial*: SEG, 1–30.
- Xia, J., C. Chen, G. Tian, R. D. Miller, and J. Ivanov, 2005, Resolution of high-frequency Rayleigh-wave data: *Journal of Environmental and Engineering Geophysics*, **10**, 99–110.
- Xia, J., R. D. Miller, and C. B. Park, 1999, Estimation of near-surface velocity by inversion of Rayleigh waves: *Geophysics*, **64**, 691–700.
- Xia, J., R. D. Miller, C. B. Park, J. A. Hunter, and J. B. Harris, 2000, Comparing shear-wave velocity profiles from MASW with borehole measurements in unconsolidated sediments, Fraser River Delta, B.C., Canada: *Journal of Environmental and Engineering Geophysics*, **5**, 1–13.